Comparison of Lidar Water Vapor Measurements #1 Using Raman Scatter at 266 nm and 532 nm

Ronnie Harris, Franz Balsiger, C. Russell Philbrick
Applied Research Laboratory / Pennsylvania State University
P.O.Box 30, State College, PA 16804
Phone: +814 863 8340 Fax: +814 863 8783 Email: fxb9@psu.edu

ABSTRACT

Raman lidar measurements at different wavelengths have become a well-established technique to obtain water vapor profiles. Measurements of the atmospheric distributions of water vapor have been made with the LAMP lidar (Laser Atmospheric Measurement Program) during the 1995 Case I measurement program on Wallops Island, VA. The simultaneous measurements obtained from the vibrational Raman technique at night using the visible signal ratio of 660/607 nm and the ultraviolet signal ratio of 295/285 nm were compared in order to validate the Raman technique for the UV channel. Correlations of the water vapor between the visible and UV channel were made, producing an overall average correlation of 0.94. Data sets with detailed vertical night time profiles from the surface to 4 km are presented. In addition, daytime vertical profiles from the surface to about 1 km are also shown.

INTRODUCTION

Water vapor, one of the most variable constituents in the atmosphere, has a major influence on the Earth's energy budget and climatic system. For instance, changes in the Earth's climate may occur when tremendous amounts of energy are transferred into the atmosphere in the form of latent heat as water evaporates and when energy is extracted from the atmosphere in the form of sensible heat as water vapor condenses [1]. Also, water vapor participates as a dominant "greenhouse" gas by absorbing and trapping the radiation that is remitted by the Earth particularly in the 5 to 7 μm spectral region [2]. Because of water vapor's important role, an understanding of its spatial and temporal distribution in the atmosphere is needed to obtain knowledge of many of Earth's atmospheric processes. Some of the most commonly used methods of measuring water vapor are radiosondes, satellite observations, meteorological towers, and remote sensing instruments, such as DIAL and Raman lidars [3].

In particular, the Raman lidar technique has exhibited the ability to produce high spatial and temporal resolution measurements of water vapor, however, most of these measurements are limited to nighttime operations. Daytime operations are difficult because of the high background of solar radiation. A solution to this problem is to operate with wavelengths in the "solar blind" spectral region between 230 and 300 nm [4]. This technique is based on the principle, that stratospheric ozone absorbs most of the solar radiation between 230 and 300 nm in the Hartley band and wavelengths in the Higgins bands which extend to 340 nm [5]. A disadvantage to operation in this spectral region is that absorption by tropospheric ozone and strong molecular scattering will limit the transmission path of the laser light. Therefore a correction for the attenuation of the laser light by ozone absorption must be applied when operating with wavelengths between 230 and 300 nm.

In this paper, we will discus the correction that is applied to the water vapor measurements to account for the attenuation of the laser light due to the wavelength dependence of molecular (Rayleigh) scattering. In addition, there will also be a discussion about the correction that is needed for the UV channel because of the difference in absorption of the water and nitrogen lines due to ozone in the Hartley band. Then, simultaneous measurements of water vapor profiles for visible and UV channels will be compared. Finally data sets showing daytime vertical profiles obtained from the UV channel will be displayed and analyzed.

INSTRUMENTATION

A multi-wavelength Rayleigh/Raman lidar was built at the Pennsylvania State University in the summer of 1991. The Laser Atmospheric Measurement Program (LAMP) was developed to study the properties of the middle and lower atmosphere (0-80 km). LAMP utilizes a Nd:YAG laser that has a pulse repetition frequency of 20 Hz and a fundamental wavelength of 1064 nm. The Nd:YAG laser is doubled and quadrupled by nonlinear crystals. The laser's output energy per pulse is 1.5 J at 1064 nm, 0.6 J at 532 nm and 80 mJ at 266 nm. LAMP transmits both the 532 nm and the 266 nm wavelengths. The system contains a f/15 Cassegrain telescope which collects the backscattered signal and sends it over a fiber optic cable to a detector box. LAMP's detector box measures the vibrational Raman backscatter return from H_2O, N_2 and O_2 in the UV at 295 nm, 284 nm and 277 nm, respectively, with photon counting photo multiplier tubes (PMT). In the visible it measures the vibrational Raman return of H_2O and N_2 at 660 nm and 607 nm, respectively, and the rotational Raman return at 528 nm and 530 nm with photon counting PMT's and the Rayleigh backscatter return at 532 nm with an analog detector. LAMP's coaxial configuration allows for near field as well as far field measurements.

From September 9 to September 22, 1995, LAMP participated in the CASE I program on Wallops Island, VA. During the program, coincident measurements of atmospheric structure properties and water vapor and ozone distributions were made by several different instruments. The NASA/GSFC (Goddard Space Flight Center) Raman water vapor lidar was among those instruments which were included in the measurement program. There were also a series of radiosondes and ozone sondes

0-7803-3068-4/96$5.00©1996 IEEE

launched by the staff at NASA Wallops. Also the NASA/LSFC aircraft water vapor lidar experiment, LASE, had overflights on several occasions during the campaign. The data from each of these instruments is intended to be used in cooperative investigations between the various groups.

DATA ANALYSIS

The water vapor content of the atmosphere can be expressed as the ratio of its mass to the mass of ambient dry air, known as water vapor mixing ratio (g/kg). In lidar measurements of water vapor in the visible channel, the mixing ratio is expressed as

$$w(z) = \frac{n_{H_2O}(z)}{n_{dryair}(z)} \frac{M_{H_2O}}{M_{dryair}} = K_{vis} \frac{S_{H_2O}(z)}{S_{N_2}(z)} \qquad (1)$$

where n is number density, M is molecular mass, K_{vis} is the calibration constant and S_{H_2O} and S_{N_2} are the Raman backscatter count rates for water vapor and nitrogen in the visible, respectively [6]. The nitrogen signal is used because nitrogen represents a constant portion of dry air. Taking the ratio of two neighboring wavelengths eliminates many of the unknown factors within the lidar equation, such as telescope form factor, absolute detector sensitivity and transmitted power. However, parameters that are wavelength and altitude dependent such as molecular scattering and ozone absorption, are not canceled in the ratio and must therefore be eliminated via a correction procedure.

The strength of Rayleigh scatter is proportional to the atmospheric density. As light passes though the atmosphere the loss of light due to molecular scattering over a distance z can be expressed as

$$I_\lambda(z) = I_{\lambda,0}\, e^{-\sigma_\lambda \int_0^z n(r)dr}, \qquad (2)$$

where n is the number density of air and σ_λ is the Rayleigh scattering cross section for air at the wavelength λ, given by

$$\sigma_\lambda = \frac{(3.93 \pm 0.05) \times 10^{-28}}{\lambda^{3.916 + 0.074\lambda + 0.05/\lambda}} cm^2, \qquad (3)$$

where λ is in μm [7]. This form takes the variation of the refractive index of air into account. For altitudes well below 5 km, an analytical calculation of the optical thickness can be made using (2), given the temperature T_0 and the pressure P_0 at the ground and assuming the temperature T(z) decreases linearly with altitude. Integrating the hydrostatic equation

$$\frac{dP}{dz} = -\frac{gM}{kT(z)} P(z), \qquad (4)$$

where g is the acceleration due to gravity, M is the mean molecular mass of a air molecule, and k the Boltzmann's constant, yields the atmospheric pressure P(z). Treating the air as an ideal gas, the integral of the optical thickness is given by

$$\kappa(z) = \int_0^z n(r)dr = \frac{P_0}{gM}\left[1 - \left(\frac{\alpha z}{T_0} + 1\right)^{-\frac{gM}{k\alpha}}\right] \qquad (5)$$

where α is the temperature gradient. Therefore, assuming that the molecular scattering is the only wavelength dependent attenuation, the corrected water vapor mixing ratio is given by

$$w(z) = K_{vis} \frac{S_{H_2O}(z)}{S_{N_2}(z)} e^{(\sigma_{H_2O} - \sigma_{N_2})\kappa(z)}. \qquad (6)$$

We know also that the particle/aerosol attenuation can add a wavelength dependent term, however this contribution is difficult to estimate and its contribution is generally less significant.

In the UV spectral region the absorption due to ozone must also be considered. By measuring the Raman back scatter of N_2 and O_2 it is possible to obtain the integrated ozone column density for the altitude range of interest. Similar to (1) the expression for the ozone column density is found by taking the ratio of the O_2 and N_2 Raman back scatter signal in the UV region. Applying the Beer-Lambert law leads to the following expression [8] for the integrated ozone column density

$$\frac{S_{O_2}(z)}{S_{N_2}(z)} = \frac{O_2}{N_2} e^{-(\sigma_{O_2} - \sigma_{N_2})\int_0^z O_3(r)dr}. \qquad (7)$$

Because the ratio of O_2 to N_2 is constant in the lower atmosphere (7) can be used to determine the ozone column density. The water vapor is then given for the UV channel as

$$w(z) = K_{uv} \frac{S_{H_2O}(z)}{S_{N_2}(z)} \left[\frac{S_{O_2}(z)}{S_{N_2}(z)}\right]^{-\frac{\sigma_{H_2O} - \sigma_{N_2}}{\sigma_{N_2} - \sigma_{O_2}}}, \qquad (8)$$

where S_X are the count rates at the corresponding wavelength already corrected for the losses due to molecular scattering as discussed above. K_{uv} is the calibration constant for the visible channel.

The count rates S_X at the different channels are given as the difference between the measured signal returns and the background counts for each of the channels. These quantities follow a Poisson distribution. For the calculation of measurement error we treat them as Gaussian distributed variables. This simplification leads to reasonable estimates of the measurement error. In (6) and (8) the only critical term in the error propagation is the division by S_{N_2}. For $S_{N_2} < 5$ counts larger differences between the exact and the simplified technique would occur in the error estimation. Since we only look at data were S_{H_2O} is bigger than 1 count and S_{N_2} is more than one order of magnitude larger

than S_{H_2O} the critical condition never occurs.

The two calibration constants K_{uv} and K_{vis} can be obtained by comparing the uncalibrated lidar profile with a profile from a balloon sonde. For each lidar range bin we ratio the balloon water vapor with uncalibrated lidar value and take their weighted average.

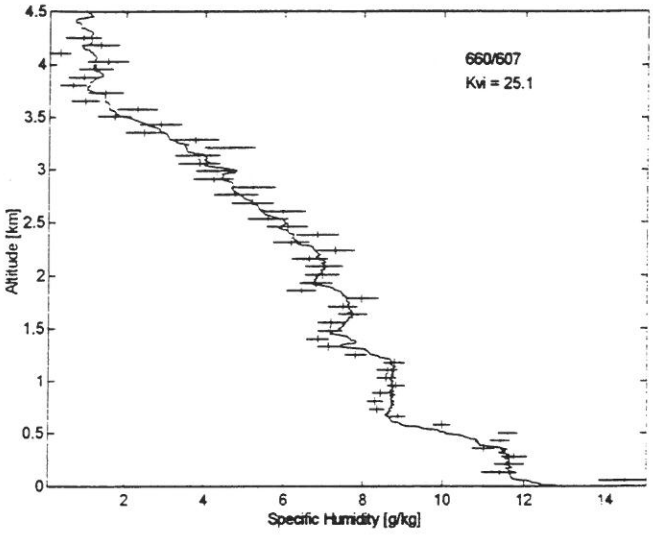

Figure 1. Vibrational Raman lidar water vapor profile together with a concurrent radio sonde profile.

MEASUREMENTS

Figure 1 displays a comparison water vapor mixing ratio measurements obtained by LAMP and a concurrent radiosonde released 3 km away from the lidar site on September 18, 1995 at Wallops Island around 02:45 UT. The lidar profile was integrated over 30 min and has a height resolution of 75 m. A comparison of the lidar and the radiosonde profiles show that their fine structures have similar characteristics, thereby, showing that measurements between both instruments are consistent. Between ground and 2.5 km both instruments reveal the same detailed layer structure.

The left panel of Figure 2 provides examples of water vapor profiles measured by both the UV and the visible channels integrated over 60 min starting at 01:20 UT on September 16, 1995. On the right panel the correlation between the two measurements is displayed. Both the profiles are in good agreement up to 2 km. The correlation coefficient of the two measurements is 0.97. The good correlation between the two methods validates the data analysis for the UV channel and shows that the technique can be used for daytime measurements.

Figure 3 shows an example of a UV water vapor daytime measurement and a concurrent radiosonde profile. The lidar profile was taken on September 20,1995 at 19:25 UT using 30 min integration. The balloon was released at 19:38 UT, 3 km away from the laser site. The reduced range of the daytime measurement is due to difficulties in aligning the laser beam in the field of view of the telescope when the daylight background was present. In the present setup of the LAMP instrument we have to rely on the alignment of the prior night. Due to the low background level in the UV, one can expect to have a similar performace during daytime as during nighttime (see Figure 2) with a correct alignment.

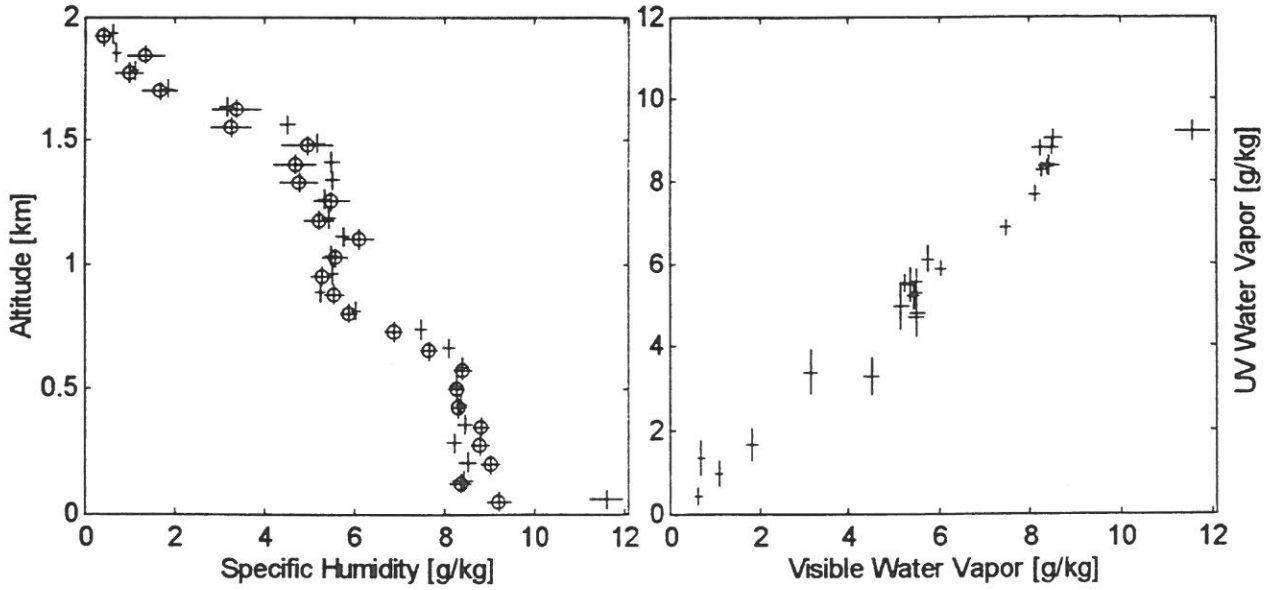

Figure 2. Comparison of a visible and a ultraviolet (circles) profiles. The bars indicate the measurement uncertainty. The right panel showa the correlation between the two, the correlation coefficient is 0.97.

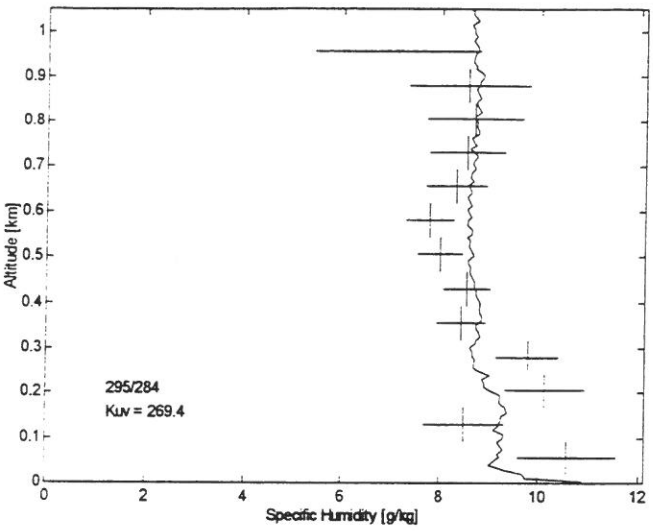

Figure 3. Daytime vibrational Raman water vapor profile from the UV channel togther with a concurrent radio sonde profile.

CONCLUSIONS

The methods of using corrections for the molecular scattering wavelength dependence and the corrections of the profile for tropospheric ozone scattering have been demonstrated. We have shown that using the vibrational Raman return from a 266 nm pulsed beam at 295 nm, 284 nm and 277 nm provides a valid technique to measure water vapor profiles in the lower troposphere. Daytime measurements were performed with this technique. However, to improve the daytime measurements it is necessary to make the system's alignment more stable with respect to time.

ACKNOWLEDGMENTS

Support for this project has been provided by Dr. J. Richter, NCCOSC/RDTE. The experiment was made possible through a collaborative effort with Dr. G. K. Schwemmer, NASA/GSFC. The work of F. Balsiger was sponsored by the Swiss National Science Foundation. We thank Frank Schmidlin, NASA/GSFC Wallops Island, for providing the rawinsonde data. We thank S. Mathur, M. O'Brien, G. Pancoast and T. D. Stevens for the help during the campaign.

REFERENCES

[1] J. P. Peixoto, and A. H. Oort, Physics of Climate, American Institute of Physics, New York, 1992.

[2] S. C. McKinley, Water Vapor Distribution and Refractive Properties of the Troposphere, MS Thesis, The Pennsylvania State University, 1994.

[3] S. H. Melfi and D. Whiteman, "Observations of Lower Atmospheric Moisture Structure and Its Evolution Using Raman Lidar", Bulletin American Meteor. Society, vol 66, no 10, pp 1288 - 1292, 1985.

[4] R. M. Measures, Laser Remote Sensing, John Wiley and Sons, New York, 1990.

[5] T. G. Kyle, Atmospheric Transmission, Emission and Scattering, Pergamon Press, Terrytown NY, 1991.

[6] S. Rajan, T. J. Kane, and C. R. Philbrick, "Multiple-wavelength Raman Lidar Measurements of Atmospheric Water Vapor", Geophysical Research Letters, vol.21, no. 23, pp 2499-2502, 1994.

[7] M. Nicolet, R. R. Meier, and D. E. Anderson, Jr. "Radiation Field in the Troposphere and Stratosphere II. Numerical Analysis", Planet. Space Sci., vol. 30, no. 9, pp 935-981, 1982.

[8] D. Renault, J. C. Pourny, R. Capitini, "Daytime Raman-lidar measurements of water vapor", Optics Letters, vol. 5, no. 6, pp 233-235, 1980.